Micro-valve with in-plane fluidics using surface channel technology on SOI wafer for use with micro-Coriolis sensor

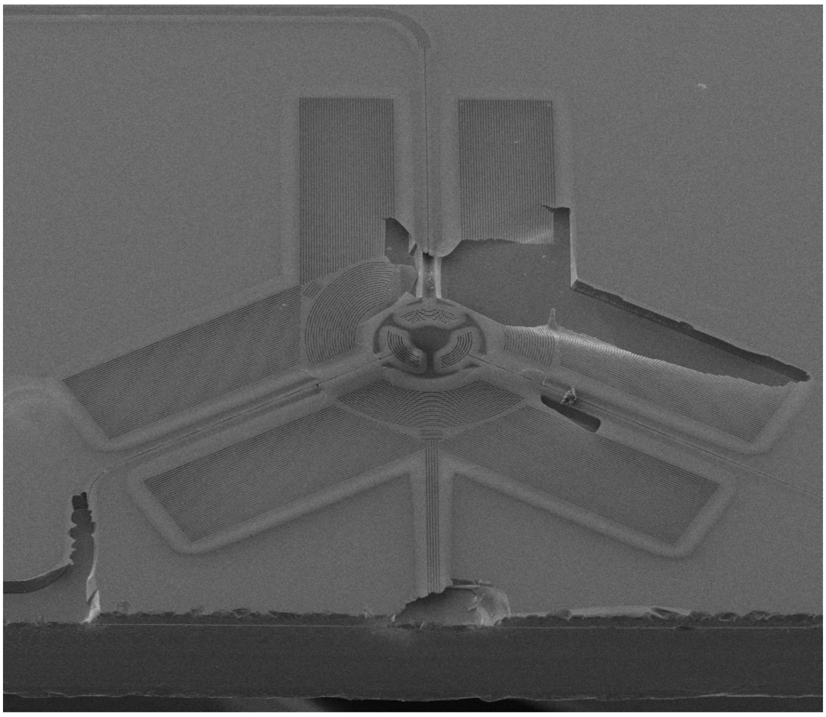

UNIVERSITY OF TWENTE.

Author:
Esken Meutstege

Supervising committee:
Prof.dr.ir. Gijs Krijnen
Dr.ir. Remco Wiegerink
Dr.ir. Dannis Brouwer
Dr.ir. Joost Lötters
Jarno Groenesteijn MSc
Maarten Groen MSc

May 13, 2014

Contents

Abstract

Research, design and fabrication of a micro-valve for the micro-Coriolis mass flow sensorusing surface channel technology. The ultimate goal is to make a micro-valve on a SOI wafer where the fluidics are completely in-plane using surface channel technology. The advantage of the in-plane fluidic design is that no external connectors have to be used for connection to and from the micro-valve. The micro-valve can therefore be integrated directly next to a micro-Coriolis mass flow sensor within the same process flow. The design of the micro-valve consists of two types, one is the proof of concept for the functioning of the micro-valve and the other is the actual in-plane fluidic micro-valve.

The micro-valves are modelled in COMSOL and simulated to determine the dimensions of the micro-valves, so the stress levels in the micro-valve suspension stay within a safe region. To get an estimate of what the fluidic characteristics are the resistance of the channels and the valve are determined using COMSOL and analytical calculations. This proofs that the valve itself has the dominant resistance, so the valve can be used to control the flow. With the dimensions known the masks for fabrication are designed. The cavities under the membrane are created using surface channel technology. After the fabrication process the results are analysed to optimize the masks. In the first fabrication run non of the wafers could be finished due to machine and process problems. So by optimizing the masks and the process flow the future fabrication runs should have a better yield.

1 Introduction

In this thesis a micro-valve is designed for the micro-Coriolis mass flow sensor [1]. To be able to integrate the micro-valve on the chip of the micro-Coriolis mass flow sensor the process flow has to be virtual the same. Using a Silicon On Insulator (SOI) wafer and surface channel technology [2] [3] a micro-valve can be created where the fluidic channels stay in-plane with the wafer. Most of the micro-valves in literature are made up of wafers that are bonded together [4] to create a valve. But as the goal is to integrate the valve into the process of the micro-Coriolis mass flow sensor, it has to be done within the same wafer without bonding. By using bonding the process has to be completely altered. Also the inlets and outlets are in most designs at the bottom and/or the top [5] as can be seen in the top and middle part of figure 1.1. The advantage of the micro-valve in this thesis is that the fluidic channels stay in the wafer, like it is shown in the bottom of figure 1.1. So the fluidic channels are in-plane with the wafer and no connections to the outside world have to be made.

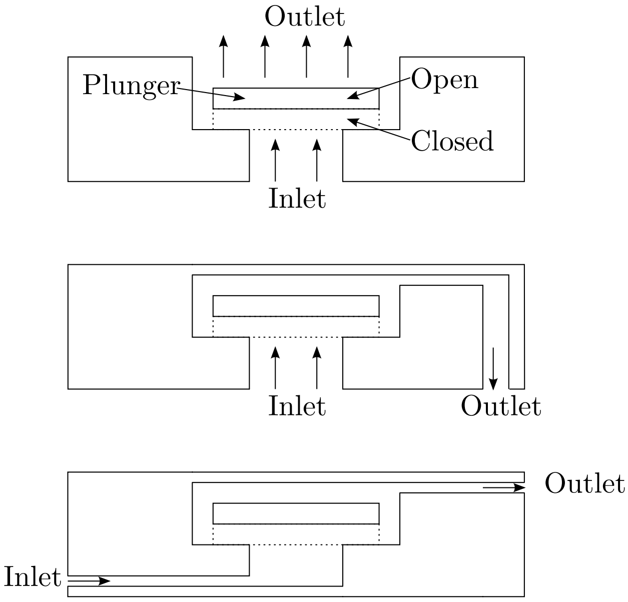

Figure 1.1: Top: inlet at bottom and outlet at top. Middle: Inlet and outlet on bottom. Bottom: inlet and outlet in-plane.

The advantage of using the in-plane fluidic micro-valve is that less chip space is needed for interconnection and the valve can be directly integrated next to the micro-Coriolis mass flow sensor. So the dead volume is greatly reduced between the valve and the micro-Coriolis mass flow sensor. Normally the valve is made with a totally different process. This is schematically shown in figure 1.2

With multiple valves as shown in figure 1.2 one can even switch between different types of media. When the valve can be controlled accurately it should be even possible to make a control loop, with the micro-Coriolis mass flow sensor as sensing element and the in-plane fluidic valve as actuator. When the flow is controllable also mixing of different media is possible. So a very compact micro-valve is created that can be used in-line without adding extra complexity of external fluidic connections.

For this research several different valve types are designed, so the functioning of the valve can be characterized. The aim is to create a micro-valve and to research if the valve can be actuated in such a way the flow through the valve can be controlled. The full scale mass flow of the micro-Coriolis mass flow sensor is in the range of $1\,\mathrm{g\,h^{-1}}$, so to be useful as controller valve the

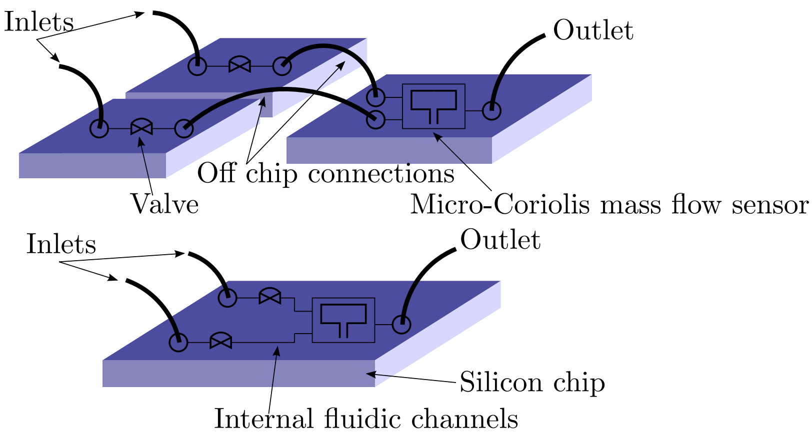

Figure 1.2: Top: Two micro-valves connected to the same micro-Coriolis mass flow sensor. Bottom: Two integrated in-plane fluidic micro-valves on a micro-Coriolis mass flow sensor chip.

flow through the valve should be in this range.
This thesis starts with explaining the geometry of the micro-valves in more detail. Then the stress and stiffness are analysed for the membrane that is used for suspension of the plunger. Another important factor is the fluidic characteristics of the micro-valves which is treated in the next chapter. The following chapter is about the actuation of the micro-valve. Now that all physical parameters are determined the masks for fabrication are discussed, followed by the fabrication process and the problems that have occurred. For further characterisation a measurement plan is discussed. And as final chapter the conclusion and recommendations for improvement for future work.

2 Geometry

The most important part of the micro-valve is the membrane that suspends the plunger. The membrane is a thin layer of Silicon-Rich-Nitride (SiRN) that is put on top of the silicon. Making small holes called slits in the SiRN layer the silicon underneath can be etched away. Making use of the slit pattern the device layer can be shaped with large or small patterns. The device layer is used to create the plunger by etching away the surrounding silicon and leaving the shape of the plunger intact. The silicon is etched away till the Buried OXide (BOX) layer is uncovered. By completely etching away the BOX layer underneath the plunger a free hanging plunger is created suspended by the SiRN membrane. The handle layer therefore becomes the seat of the valve. The plunger and the suspension membrane can now be used to open or close the channel underneath the plunger. The slits for etching the silicon underneath are closed again by growing a new layer of SiRN. The new layer SiRN will also cover all the inside walls of the valve, so the whole valve becomes more chemical resistant.

2.1 Backetched (BE) Valve

In figure 2.1 an impression of the valve is shown. As a proof of concept a very basic micro-valve is created. The back etched holes shown at 4 in the handle layer at number 1 are used for fluidic connections to characterize the micro-valve during measurements. The most easy way to proof the micro-valve concept is working is making the inlet under the plunger, which is number 2 of the micro-valve. The area around the plunger where the silicon is etched away will be referred to as the outer cavity. To prevent high stress in the membrane from the inlet pressure, the inlet is chosen to be under the plunger instead of in the outer cavity. From the outer cavity a wide channel, number 5, is made to the outlet hole, which is also created using a backetch. The plunger is designed to be round so the membrane, which is shown at number 3, can uniformly bend down with the plunger. Sharp corners have higher stress concentrations, which could result in tearing the membrane. The diameter of the plunger is designed to be 500 µm, so a small cylindrical magnet could be glued on top of the plunger. The magnet could be used to actuate the valve with a coil.

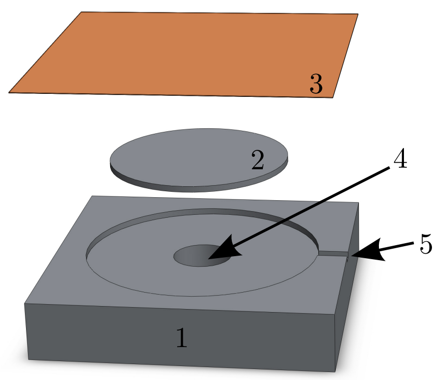

Figure 2.1: The BE valve type taken apart. 1) Handle layer. 2) Valve plunger. 3) SiRN top layer. 4) Back etched hole. 5) Output channel.

Looking at figure 2.2 the medium inlet is at the bottom of the valve. When the plunger is open the medium can flow through the radial channel between the plunger and the seat towards the outer cavity. Then the medium can flow from the outer cavity into the wide channel that connects to the backetched hole. The outlet has to be far away from the inlet hole, because else the fluidic connectors on the backside don't have enough room to be glued on the substrate and create a good seal.

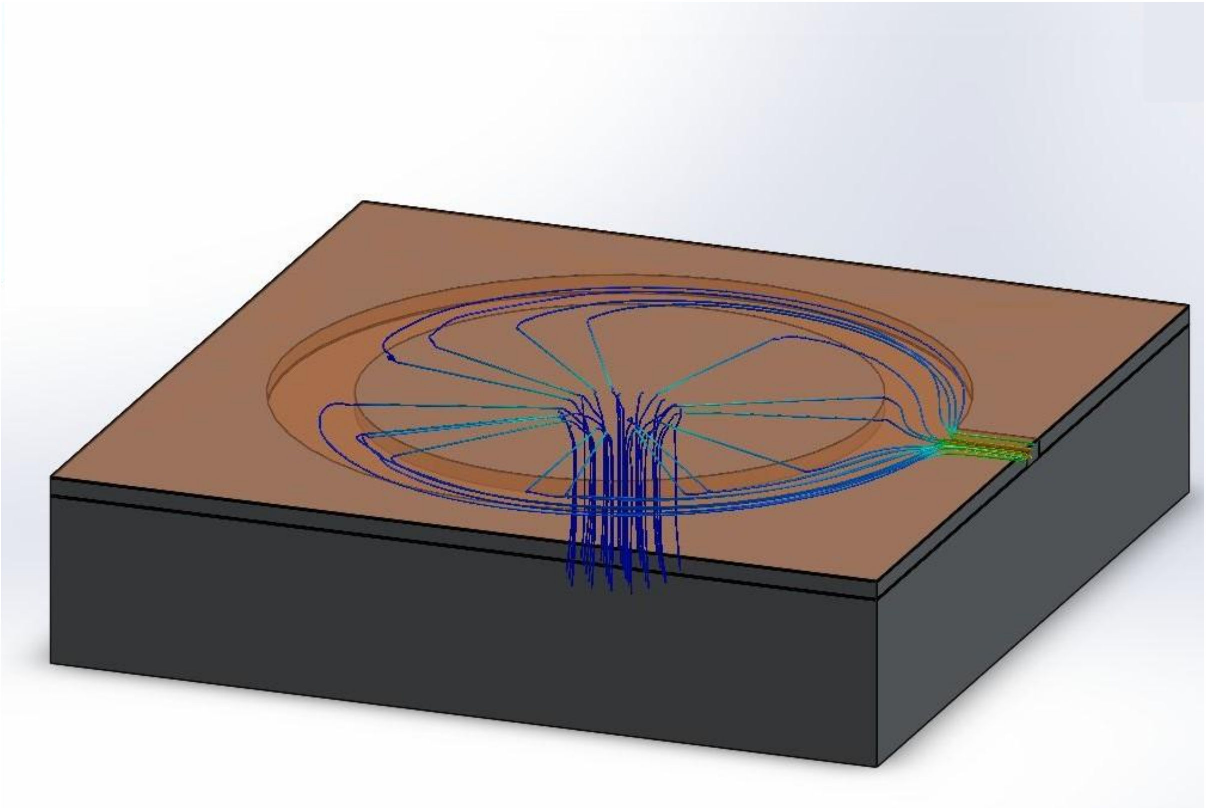

Figure 2.2: Solidworks FloXpress simulation of the flow

2.2 In-plane (IP) Valve

The second type of micro-valve is the preferred in-plane fluidic micro-valve. In the previous BE valve type the inlet is under the plunger, so the fluidics are not completely in-plane. So instead of making the inlet under the plunger, the inlet is made in the plunger. Using the slits again a cavity in the plunger itself is created. This inner cavity has to be connected to the inlet by means of a channel. The channel has to cross the outer cavity, so a tube inside a tube is created. In figure 2.3 the tube in a tube concept is shown. Where the outside tube pointed out with number 2 is the outer cavity and the inside tube with number 1 is the inlet tube crossing the outer cavity. The inside tube is a free hanging structure, so it can bend easily.
The IP valve concept is shown in figure 2.4. To make sure the plunger is guided straight when actuated several connection tubes are added to create a symmetrical structure. The design therefore is arranged as a star with 3 tubes to make it symmetrical with the least tubes. More tubes means that the stiffness of the complete structure will increase, which means more force is needed to actuate the plunger. Also the membranes between adjacent tubes become smaller, so higher stresses are induced in those membranes when bended.

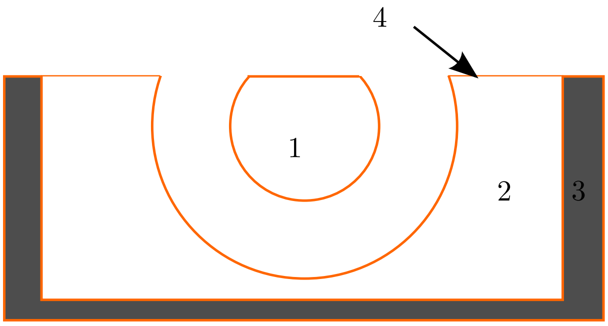

Figure 2.3: Cross-section view of the tube in a tube concept 1) Inlet tube 2) Outer cavity ”tube” 3) Silicon 4) SiRN layer.

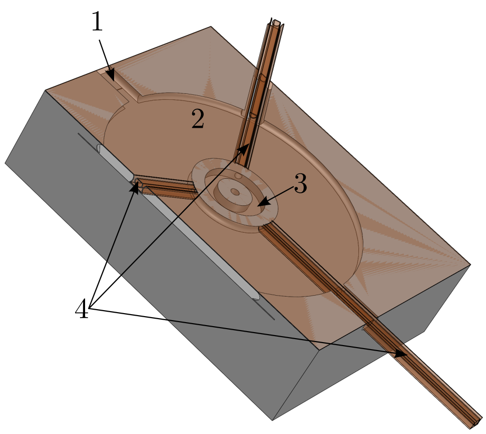

Figure 2.4: The IP valve design using symmetrical connected inward tubes. 1) Connection outer cavity 2) Outer cavity 3) Inner cavity 4) Tube in a tube connections of the inner cavity.

3 Membrane stress and stiffness

The membrane is an important part of the design, because it is the suspension of the plunger and also the seal of the outer cavity. To get an understanding of what the limits should be using different dimensions of the valve, a few simulations are done using Finite Element Method (FEM) analyses with COMSOL Multiphysics [6].

3.1 Stress in the membrane

A simplified model of the valve is used. The used model is shown in figure 3.1. The model is axis-symmetric around the middle of the plunger, which is pointed out with number 2. The pressure of the fluid or gas at number 5 is projected on the inside of the membrane, which is number 3. At number 6 the force/displacement is put on the plunger side and can move freely with respect to the part with number 1, which is the fixed part of the valve.

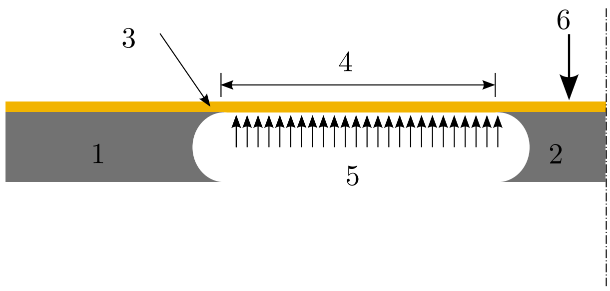

Figure 3.1: Axis symmetric simulation model with 1) Fixed layer 2) Plunger 3) Membrane 4) Width of the membrane 5) Pressure under the membrane 6) Force/displacement on plunger

According to literature [7] the fracture stress SiRN can handle is in the range of 900 MPa. But due to imperfections in the crystal lattice and stress due too different expansion coefficients of the materials a lower induced stress on the membrane can eventually also break it. The maximum stress is therefore set for 300 MPa to be sure the membrane doesn't break during operation.

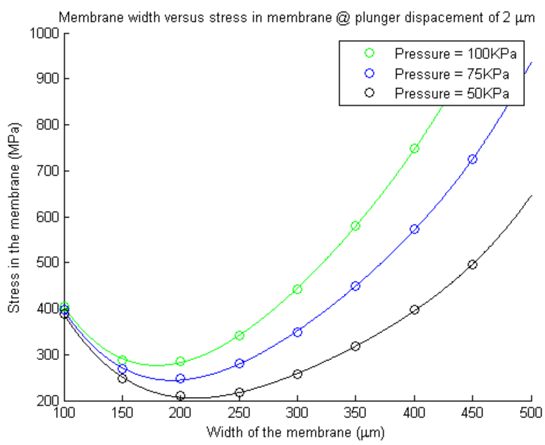

Figure 3.2: Simulation results for the width of the membrane versus the stress

The result of simulating a displacement of 2 μm and the resulting stress in the membrane is shown in figure 3.2. The simulation is done for three different pressures under the membrane.

One can see that around a membrane width of 200 µm the lowest possible stress is achieved. At small membrane widths the stress becomes higher, because the membrane can bend only over a small length. But at large membrane widths the total force on the membrane due to the medium pressure increases, because the surface area increases. So the pressure forces the membrane to become convex and extra stress is induced in the membrane. An optimum can be seen in figure 3.2 where the bending from the membrane and the area of the membrane are combined on their lowest.
To get an idea of the actuation force that is needed to actuate the valve a simulation is done including the medium pressure in the outer cavity. The medium pressure is an important factor to take into account, as seen before with the stress in the membrane. For a wider membrane the force that is needed to close the valve is also higher. The result of the simulation is shown in figure 3.3. The valve will have a maximum deflection of 2 µm, which has a stress of less than 300 MPa and a force of approximately 24 mN.

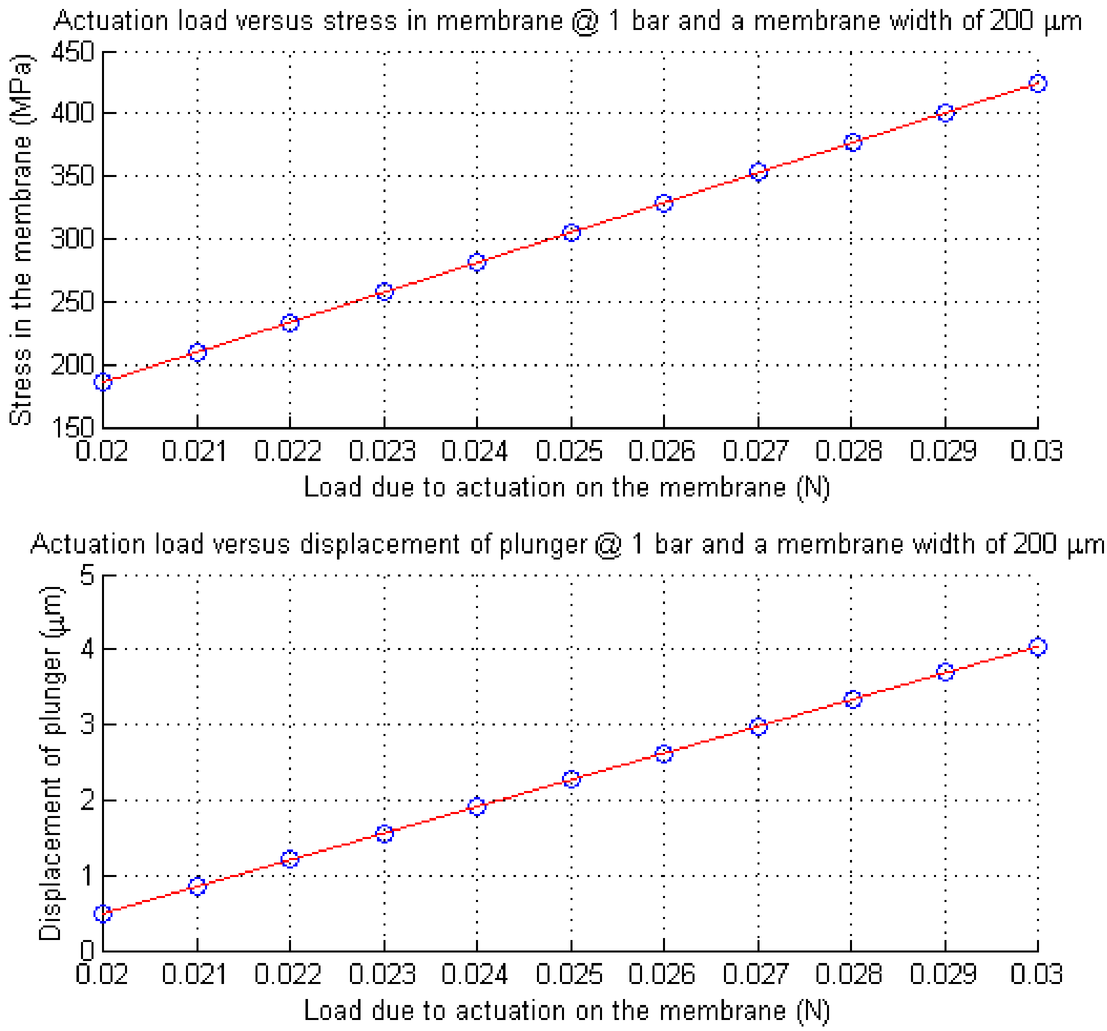

Figure 3.3: The top graph shows the maximum stress on the membrane for different loads, whereas the bottom graph displays the displacement of the plunger for the actuation load.

3.2 In-plane valve

3.2.1 Connection Tube

The tube in a tube concept that connects the inner cavity with the rest of the chip is also simulated. The tube is hanging free and is only fixed at the beginning and the end. The cross section of the used tube has a flat top. The top is flat because of the used process. The results of the simulation are shown in 3.4. The round tube type has lower stress for tube lengths till 1500 µm. To stay beneath the limit of the maximum stress a minimum tube length of 800 µm has to be used when the plunger displacement is 2 µm. But when the plunger is pulled open actively a displacement of 5 µm is possible, so then a length of 960 µm is needed. Taking a length of 1000 µm should be safe to operate the tube for closing and actively opening the plunger. Making the tube longer will increase the needed chip space. But also the area of the membrane increases, which means higher forces due to the pressure underneath.

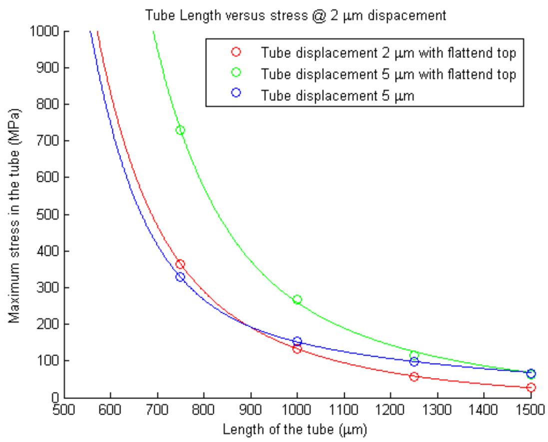

Figure 3.4: Simulation results of the stress for the free hanging connection tube

Because the connection tube that goes to the inner cavity has to pass the membrane a tube in a tube concept is created. The inner tube is surrounded by another tube so that the inner tube is hanging free to bend when the valve is actuated. The outer tube which is like a mantle has to be simulated to, but is integrated with the membrane itself. Because of the complexity of the tube in a tube concept the whole membrane is simulated with the mantle attached to it. To reduce the stress in the membrane itself a different type of suspension is also simulated to compare the results. The normal type is fixed to the silicon at the top, whereas the "mushroom" type which is conceptually shown in figure 3.5, is suspended by an extra membrane that is fixed to the bottom instead of the side wall and can move horizontal. The idea of the "mushroom" design is that the tension in the membrane is lowered, because it can also bend sideways. The results of the simulation is shown in figure 3.6. The simulations show that there are higher internal stresses for the "mushroom" design. These higher stresses concentrate at the folded corners of the design. So after these simulations the "mushroom" design is not further used for the design for fabrication.

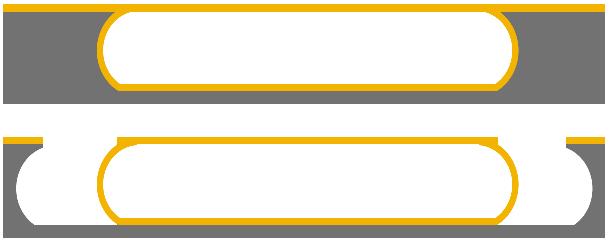

Figure 3.5: The top picture shows a normal membrane, the bottom picture is the mushroom membrane which is not fixed at the side wall.

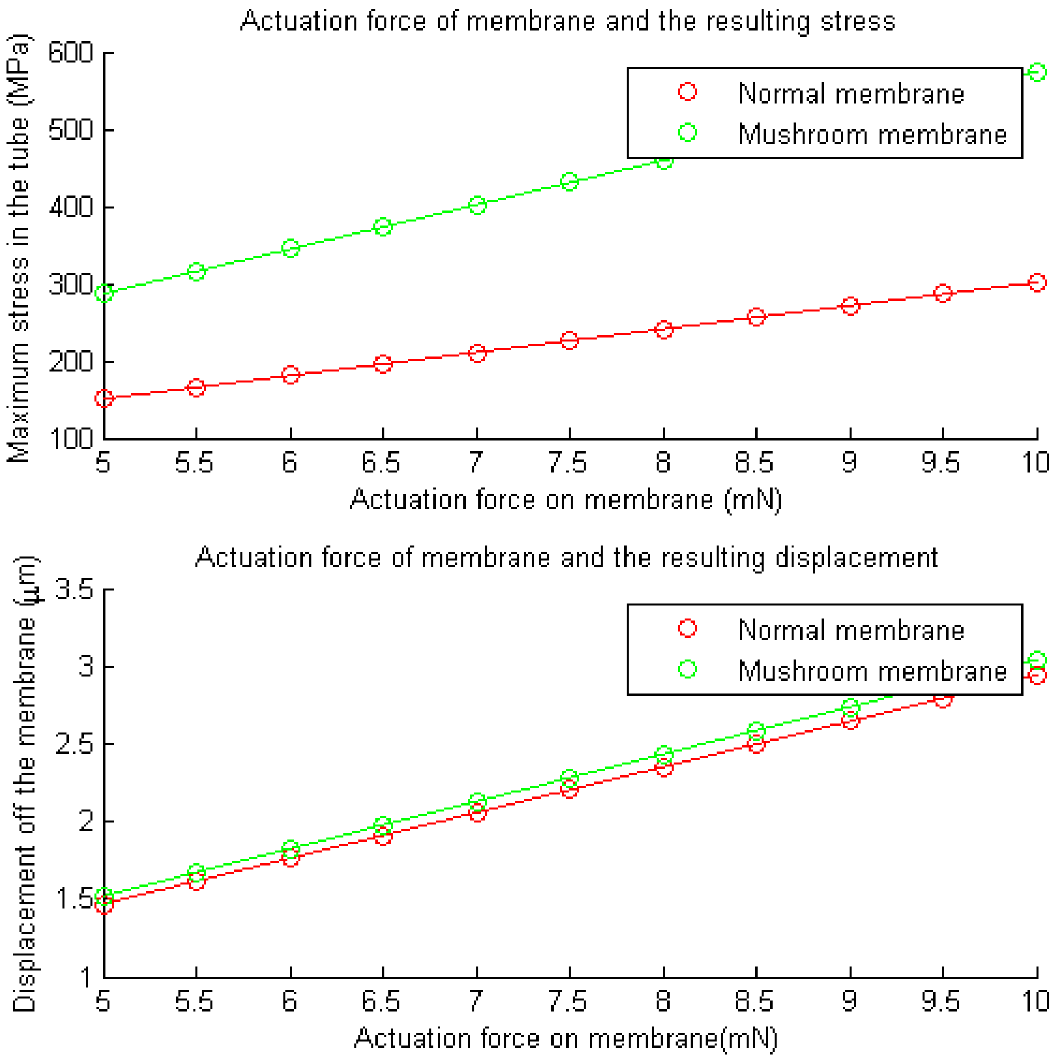

Figure 3.6: Simulation results for the stress and displacement of the membrane including the mantle of the tube in a tube design.

4 Fluidics

A model is made to investigate the fluidic characteristics of the valves. Nitrogen is used as medium for finding the characteristics, because nitrogen will also be used during measurements of the valves. In table 4.1 the parameters can be found that are used for the calculations. Where ρ is the density of the medium, μ its dynamic viscosity, $\dot{m}$ the target mass flow when opened.

ρ	$1.145\,\mathrm{kg\,m^{-3}}$
μ	$17.81 \times 10^{-6}\,\mathrm{Pa\,s}$
$\dot{m}$	$1\,\mathrm{g\,h^{-1}}$

Table 4.1: Parameters of nitrogen for fluidic calculations.

To compare the different parts of the valve the resistance of the channels is determined. The resistance is characterized by

$$R_h = \frac{\Delta P}{Q} \tag{4.1}$$

Where R_h ($\mathrm{N\,h\,m^{-5}}$) is the resistance, ΔP ($\mathrm{N^2\,m^{-1}}$) is the pressure difference and Q ($\mathrm{m^3\,h^{-1}}$) the volume flow rate. From the volume flow rate the mass flow $\dot{m}$ ($\mathrm{kg\,h^{-1}}$)rate can be calculated using the density ρ ($\mathrm{kg\,m^{-3}}$) of the fluid or gas by

$$Q = \frac{\dot{m}}{\rho} \tag{4.2}$$

So the resistance can also be written as

$$R_h = \frac{\rho}{\Delta P \dot{m}} \tag{4.3}$$

In the ideal case the radial channel created by the seat and plunger has to have the highest resistance in the fluidic system. The inlet and outlet mass flow can't choke the flow. When the plunger is then closing or opening only a part of the flow is controlled. After a certain point the mass flow can't increase more, because the inlet or outlet doesn't allow a higher mass flow to pass.

4.1 Channel characteristics

For the pressure drop over the channels that connect the inner cavity it is assumed that the tubes have a circular cross section without the flattened top. To get a better estimate for the round tube with flattened top the hydraulic diameter is used

$$D_H = \frac{4A}{P} \tag{4.4}$$

Where A is the area and P the wetted perimeter. The hydraulic diameter for one channel is $D_H = 34.2\,\mu\mathrm{m}$ instead of a round tube with diameter of $40\,\mu\mathrm{m}$.
For the case of the 5 slits wide channel the hydraulic diameter can also be calculated. The middle of the slits are $10\,\mu\mathrm{m}$ separated from each other. According to observations during fabrication of the channels they are almost $50\,\mu\mathrm{m}$ deep. Assuming the depth of $50\,\mu\mathrm{m}$ is the deepest point of the channel an estimate can be made for the hydraulic diameter.
In figure 4.1 the SEM image is shown of experiments of the surface channel technology for 5 parallel channels of $1.2\,\mu\mathrm{m}$ wide slits separated by $10\,\mu\mathrm{m}$. The results for the height of the surface channel technology measurements are shown in figure 4.2.

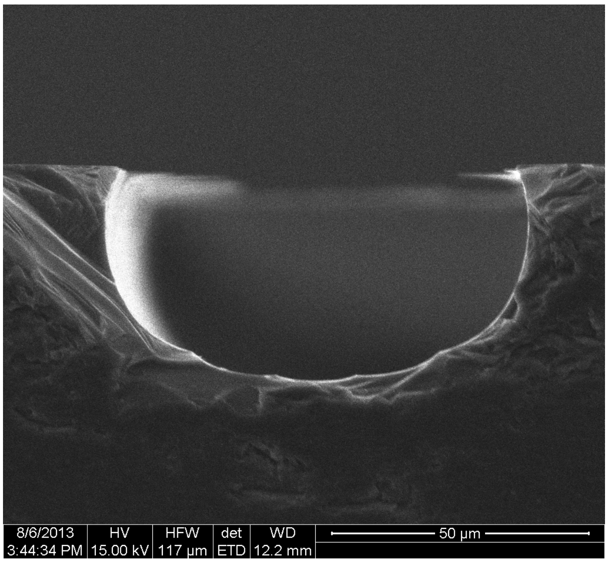

Figure 4.1: SEM image of channel width experiment for 5 slits wide channels with 10 µm spacing between rows.

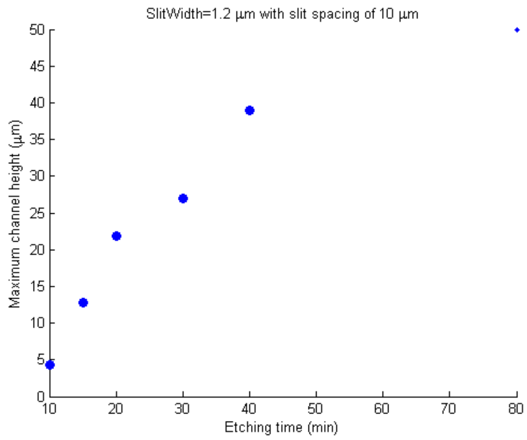

Figure 4.2: Height of the channel for 10 µm spacing between the 5 slit wide rows for different etch times

When the etching time increases the speed of the depth of the channel decreases. At the used etching time of 80 min the height should be around 50 µm. Assuming it will not touch the BOX layer, so the BOX is not removed during fabrication.
Looking at figure 4.3 the width should become 100 µm after extrapolation of the trend. Assuming the etching becomes isotropic because of the large loading inside the channel, the shape of the channel remains the same as does the aspect ratio. This assumption looks plausible with the results of figures 4.2 and 4.3. Using these assumptions the perimeter and the area can be determined, which are 271 µm and 4400 µm respectively.
Using the hydraulic diameter in the Hagen-Poiseuille equation [8] gives

$$\triangle P = \frac{128\mu L Q}{\pi D_H^4} \tag{4.5}$$

Where $\triangle P$ is the pressure difference, μ is the dynamic viscosity, L is the length of the channel,

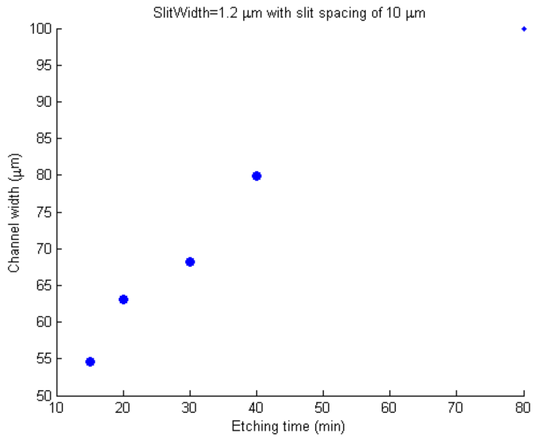

Figure 4.3: Width of the channel for 10 µm spacing between the 5 slit wide rows for different etch times

Q is the volumetric flow rate and D_h is the hydraulic diameter of the channel.
Substituting equation 4.5 in equation 4.3 for the resistance gives

$$R_h = \frac{\triangle P}{Q} = \frac{128\mu L}{\pi D_H^4} \tag{4.6}$$

To be able to calculate the resistance the length of the channel is important. Each channel section has its own length, which is shown in figure 4.4 for the IP valve.

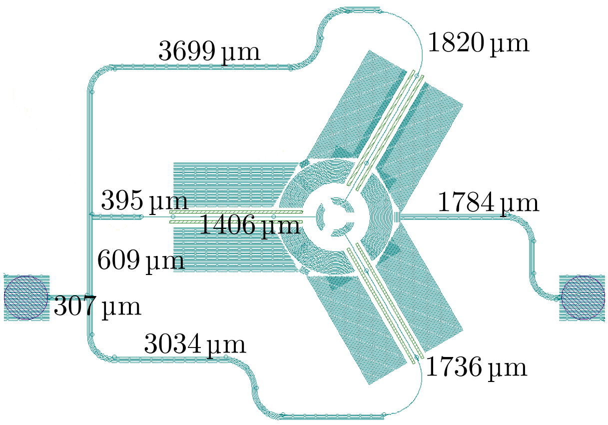

Figure 4.4: Channel length of the IP valve design

In figure 4.5 the equivalent electrical circuit is drawn for the in-plane fluidic valve. The unit of the resistance is $\mathrm{N\,h\,m^{-5}}$.
Besides the length of the channel the hydraulic diameter is also very important. Comparing the design in figure 4.4 with figure 4.5 the resistors R_1 through R_5 are the 5 slits wide channels and R_6, R_7 and R_8 are the 1 slit channels. Now the equivalent inlet resistance, which are the inlet channels before the IP valve, can be calculated by

$$R_{in,IP} = \Big((R_3 + R_6)//(R_4 + R_7) + R_2\Big)//(R_5 + R_8) + R_1 = 2.9360 \times 10^{11} \tag{4.7}$$

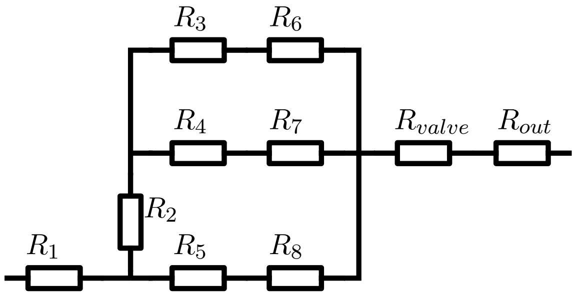

Figure 4.5: Equivalent electrical circuit of the IP valve channel resistance

The outlet resistance $R_{out,IP}$ is only determined by the 5 slit wide outlet channel which is

$$R_{out,IP} = 7.2769 \times 10^{10} \tag{4.8}$$

For the BE valve there is only a 5 slit wide output channel, which is 3880 µm long. So the output resistance is

$$R_{out,BE} = 1.5826 \times 10^{11} \tag{4.9}$$

4.2 Radial valve flow

The flow profile that is used for simulation is the channel between the seat and plunger, as is shown in figure 4.6. The inlet is situated in the middle, where in the backetch hole is situated. For the IP valve the inlet is also in the middle, but then there is a cavity in the plunger instead of the handle layer. The situating is comparable when only looking at the flow through the seat and plunger area.

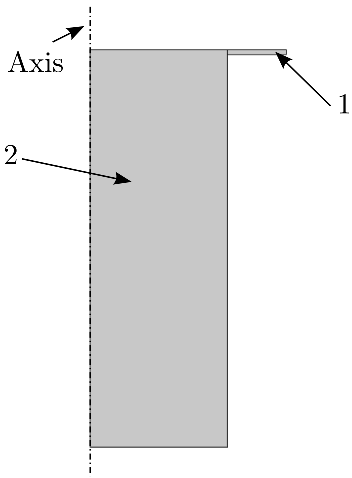

Figure 4.6: Comsol 2D axis-symmetric model of flow profile with 1) The radial flow channel between seat and plunger and 2) Half of the 350 µm wide inlet hole created by the backetch.

To validate the assumption the flow in the valve is laminar the Reynolds number, the Mach number and the entrance length have to be satisfied. Most important is the Reynolds number which is giving by

$$Re = \frac{d\rho v}{\mu} = \frac{d\rho\frac{Q}{A}}{\mu} \tag{4.10}$$

Where d is the diameter of the channel, ρ is the density of the medium, μ is the dynamic viscosity. The mean average speed of the medium is characterized by $v = Q/A$ is with Q the volume flow and A the surface area. With the backetch hole as inlet the diameter is 350 µm. The mean average speed of the inlet can be calculated as the volume flow divided by the area of the cross-section. Using the specification of a mass flow of $1\,\mathrm{g\,h^{-1}}$ and calculating from this the value for the volume flow. Filling out the values given in table 4.1 gives

$$Re = 56.7 \tag{4.11}$$

The Reynolds number is under the 2300, so it satisfied that the flow should be laminar.
With calculating the Mach number one can say something about the compressibility of the medium. The mach number is given by

$$Mach = \frac{v}{v_0} \tag{4.12}$$

In this equation v is the mean average velocity of the fluid and v_0 is the speed of sound in that particular medium. Filling out the values gives a Mach number of 0.007. When $M < 0.3$ the flow can be treated as incompressible, which means simple models can be used for calculating the flow.
Then there is the entrance length [9], which provides the distance a flow needs to become fully developed. The entrance length for the inlet is

$$Le = 0.06dRe = 1.2\,\mathrm{\mu m} \tag{4.13}$$

So one can conclude that the entrance length for the backetch hole channel, which is 500 µm long, is enough.
The flow from the middle cavity to the outer cavity has a radial pattern. For the calculation of the pressure drop the formula from the paper of Browne is used [10]. Browne comes with a formula that holds from viscous to molecular flow and the region between those. Because of the complexity of the problem the formula is very suited to make an estimation of the resistance. Rewriting the formula gives

$$R_h = \frac{\triangle P}{Q} = \frac{1}{\frac{4}{3}(\frac{\pi}{32Kn} + \frac{2\pi}{4Kn(1+2/Kn)} + \frac{1}{(1+2/Kn)})} \frac{ln(r2/r1)}{\pi h^2 v}; \tag{4.14}$$

Where $\triangle P$ is the pressure difference, Q is the volume flow rate, r1 and r2 are the inner and outer diameters of the valve ring, h is the height of the channel and v is thermal velocity of the medium. The Knudson number is defined as $Kn = \frac{\lambda}{L}$, where λ is the mean free path and L the characteristic length.
To compare the result also a COMSOL FEM simulation is done. Therefore the model in figure 4.6 is used. The space between the valve seat and plunger is only a few microns high, so this is probably the dominant part of the whole valve considering the resistance. When the resistance is determined at varies plunger positions, the flow can be set by changing the plunger position. From the backetch hole and the space between the seat and plunger a 2D axis-symmetric model is made. By using a 2D axis-symmetric model the mesh is less complex and can be set finer without creating a very large computation time, which is the case for a 3D simulation. The disadvantage is that forces orthogonal to the 2D model are not taken into account. Then the boundary conditions have to be set. The inlet is set to a pressure of 2×10^5 Pa. The outlet boundary is set to be the radial outward side of the space between the seat and plunger. The outlet pressure is set to 1×10^5 Pa.

During simulation an artifact is seen where the medium goes from the inlet hole into the radial channel. The pressure drops to almost zero as can be seen in figure 4.7. Even with the mesh made very fine or rounding the corner at that specific point the artifact remains. Looking at the total mass flow through the channel reveals that only after 10 µm into the channel it stays stable over the whole length of the channel. So the first 10 µm of the channel is not used for analysing the simulation results. This can only be done because the medium velocity is not affected and the medium doesn't flow to the low pressure point, but towards the exit of the channel. In figure 4.8 the resistance for both the simulation and calculation is shown. As can be seen the calculation of Browne and the simulation don't correspond. The calculation of Browne is a few orders of magnitude lower. When the data points are compared the difference becomes bigger for a larger opening. The big difference points out there is probably a wrong assumption made for the boundary conditions. Because nitrogen is in gas form during low pressure and room temperature the formula of Browne for the radial flow depends highly on several factors that change constantly in the channel. The difficult part is here that the channel is constantly changing its shape and therefore changing the parameters of the gas like volume, density, velocity and pressure. To make a better model for calculating the formula of Browne all these parameters have to be calculated for the different points in the radial channel. After a look at the Reynolds number for the radial channel it seems that it so high that the flow should become turbulent. With a high mass flow through a very small opening this should indeed make the conditions for turbulent flow possible. So this could also answer the difference between the simulation and calculation. The assumption that was made that all flows are laminar is therefore not valid. In future work new calculations have to be done for the case the flow becomes turbulent at the beginning of the radial channel. This could also be the problem why the mass flow is not conserved in the first 10 µm of the channel and the low pressure area that occurs during simulations with the laminar flow module. To get an idea of the resistance the opening surface of the valve should be compared with the opening of the 5 slits wide channel. The surface opening at the end of the radial channel of the valve when the seat-plunger distance is 1 µm gives 1570 µm^2. The 5 slit wide channel has a surface of 4400 µm^2, so the flow should be more choked for the radial channel meaning a higher resistance. This is for the COMSOL simulation the case, but not for the Browne calculation. Therefore the results of the COMSOL simulation seems to be the best assumption.

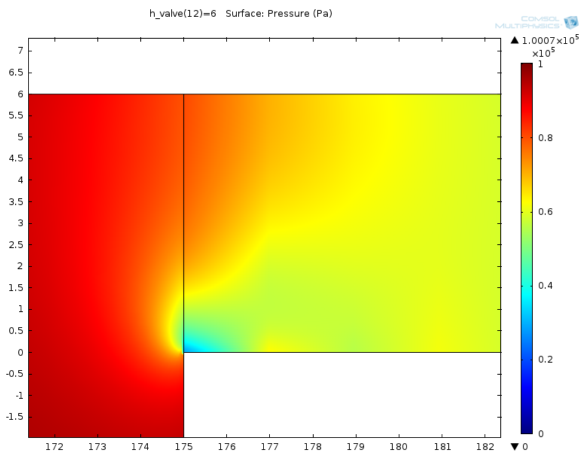

Figure 4.7: During simulation an aritfact observed at the beginning of the radial channel where the pressure drops to zero.

For a good fluidic system the resistance due to the valve opening and closing should be dominant, so when the valve is controlled, the flow is also controlled. Looking at the results of the COMSOL simulation in figure 4.8 the resistance is till a valve opening of 4 µm higher than the resistance of the in and outlet channels. But for the Browne calculation the resistance is already lower, so the valve is not controlling the flow. So for this case the valve can only be in a on or off state for the best results. So measurements of the actual valve itself can give a definite answer to this problem by actuating the valve and looking how it affects the flow.

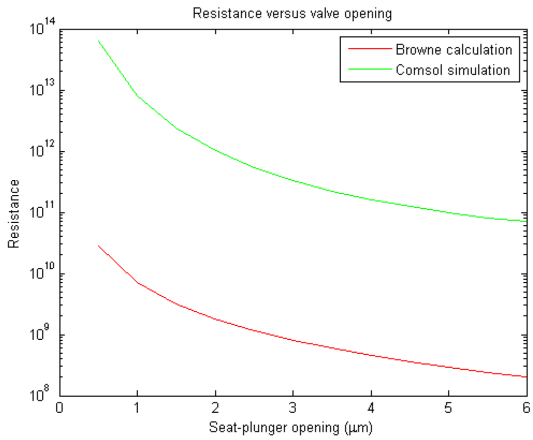

Figure 4.8: Comparison between comsol simulation and Brownes calculation method

In figure 4.9 the mass flow of the valve is shown for the COMSOL simulation with a pressure drop of 1 bar. The graph shows that the mass flow will be around $1\,\mathrm{g\,h^{-1}}$ at an opening of 2.75 µm. So when the condition that was set for a flow of $1\,\mathrm{g\,h^{-1}}$ can be satisfied by actively pulling the valve open. And so a control valve is possible for flows between zero and $3\,\mathrm{g\,h^{-1}}$ when opening the valve for 4 µm. Note that by opening the valve the same stress is induced in the membrane as for closing the valve.

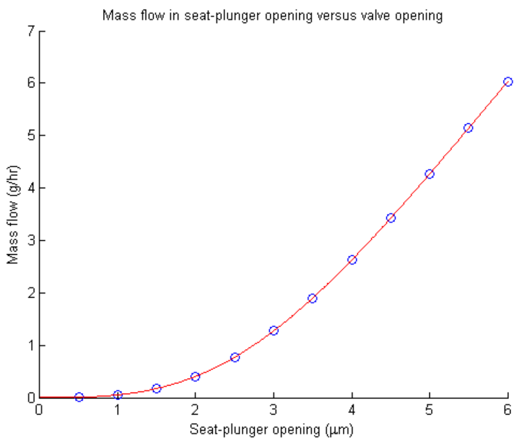

Figure 4.9: Mass flow of radial channel for different channel openings according to COMSOL simulation for 1 bar pressure difference

5 Actuation

The valves can be actuated by pushing the plunger down. For a higher flow through the valve the plunger can also be pulled actively open, but for opening it further the valve has to be glued to the actuator. In the beginning of designing the valve a look was taken at electrostatic actuation on chip. Because the working direction of the valve itself is out of plane the actuation method is less obvious. Using the plunger and seat as electrodes the valve can be closed by electrostatic forces, but opening is not possible using that method. If the valve is sticking it will not open due to the low stiffness of the membrane. So an external way of actuation has to be used. For characterising the valves an experimental measurement setup can be used. The valve can be actuated using a needle that pushes the plunger down with a piezo actuator. For pulling the plunger open the needle can be glued on top of the plunger. The needle needs to be carefully glued and can only be used in the setup. If the sample would be taken out of the setup with the needle glued on the plunger it will break because of the fragile membrane.

5.1 Coil-magnet

For the final design the actuation has to be stand alone. Because of the fragile membrane and the relative high forces the actuation has to be done preferably on the plunger itself. With magnetostatic actuation the forces can be achieved and also pushing and pulling is possible by glueing a magnet on top of the plunger and actuating it with an external coil. This way the plunger and the membrane are also isolated from external forces. So the sample can be used for experiments and can be taken out of the setup for example without damaging the membrane. Care has to be taken ofcourse that the magnet is not pulled by a metal object or other magnet. For the force between the magnet and the coil the assumption is made that the coil is also a magnet with the same dimensions. Using the results of [11] the following formula for the force can be used

$$F = -\frac{1}{2}\pi K R^4 \Big(\frac{1}{z^2} + \frac{1}{(z+2t)^2} - \frac{2}{(z+t)^2} \Big) \tag{5.1}$$

$$K = \frac{\mu_0 M^2}{2} \tag{5.2}$$

With R the radius of the magnet, z is the distance between both magnets, t is the height of the magnets and M the magnetization

The force to open/close the valve completely is around 30 mN. So the needed flux density can be calculated for the force between two identical magnets by using equation 5.2 with equation 5.1. For a flux density of 0.9 T the needed force is achieved. A permanent magnet is within this range, but a coil has to be designed that also has the needed flux density. For the magnetic field of the coil the following holds

$$B = \frac{\mu_0 N I}{L} \tag{5.3}$$

With N the number of windings, I the current and L the length of the coil.

To keep the coil small the length of the coil is taken 1 cm. For the width of the coil the wires needs to have a small diameter. But using a small diameter means also a lower current can be used. If a current is taken of 0.7 A the minimum diameter of the wire has to be 0.22 mm [12]. Then the coil needs 10 000 windings to be able to get a flux of 0.9 T. This will be a very big coil, because of the amount of windings needed. The wire diameter could be changed, but then also the maximum current has to be decreased which ends up with even more windings. By making

l_{coil}	1 cm
l_{magnet}	1 mm
radius magnet	0.5 mm
$x_{seperation,magnet-coil}$	1 mm

Table 5.1: Simulation constants for magnet and coil

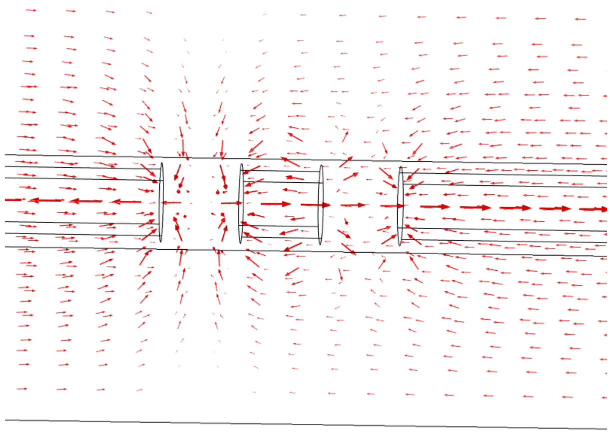

Figure 5.1: Simulation of magnet and coils showing flux density. In the middle the magnet that is glued on the plunger is shown and on the right and left a flux density in air is shown that represent the inside of the coils.

use of a material inside the coil with a high permeability the flux density can be increased, so less windings are needed. So that the coil can be made much smaller. Further research has to be done to determine if it is indeed possible to use a coil to actuate the glued magnet on the plunger.
To keep the field as uniform as possible and to create a smaller coil a second coil is put underneath the magnet. Using one coil to pull the magnet and the other to push the magnet is more efficient.
To get a more accurate model the coil and magnet are simulated in COMSOL. The coil is simply modelled as a flux density in air. The force on the magnet is then calculated. Using two coils shows that the force is more than doubled comparing it to only using one coil.
Using the the constants in table 5.1 the simulation concludes that a force of 26.4 or 30.5 mN, depending on direction of the field, with a flux density of 0.9 T is possible. See also figure 5.1 for the flux density between the magnet and the coils.

5.2 Bimorph

Another approach for actuating the valve is using a bimorph material. The bimorph material will bend, because the two materials have different expansion coefficients when heated. Also an piezo bimorph can be used which doesn't need to be heated, but driven with a voltage. The piezo is the easiest solution to implement on the design. The downside of piezo actuation is that the piezo actuator has to be rather big compared to the valve itself, but this is also the case with the magnetic actuation that is proposed earlier. When a bimorph material is used the attachment to the plunger is getting complex. The initial position can not be changed once it is glued, which is for the magnet coil principle is still possible. The magnet can freely move with the plunger when no magnetic field is applied. The advantage of using a piezo element is that it is cheaper and can be easily bought. The magnet is cheap to buy, but the coil has to be custom made so making it an expensive part.

6 Mask design

The design for the BE valve is shown in figure 6.1. At the left side the actual valve is shown with in the middle the backetch hole and around it the slits to create the membrane and the cavity beneath. From the cavity a channel is created to the outlet hole on the right. The complete hole is covered with slits, so that also here a cavity is created to have a good access to the backetch hole.

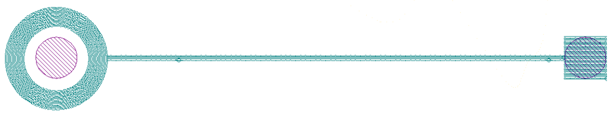

Figure 6.1: BE valve mask design, where the green is the slit mask and for the backetch the mask is shown in purple. On the left the actual valve can be seen around the backetch hole. A 5 slit wide channel runs from the outer cavity of the valve to the outlet on the right side.

The complexity of the IP valve in figure 6.2 is directly seen when compared with the BE valve. Around the plunger shown as number 5 the same membrane can be seen as for the BE valve. The membrane at number 3 is interrupted with channels coming from the outside. Each channel shown with number 7 that direct inwards is fluidic connected to the inlet hole, which is number 8 on the left side. In the middle part of the plunger also a cavity is created, in this cavity at number 4 the inlet tubes terminate. The inner cavity is divided in three parts, so that the plunger stays rigid during actuation when a needle is pressing in the middle. Also the BOX layer can be underetched in less time, because the BOX layer is removed from both inside and outside of the radial channel. On the right side the outer cavity is connected to the outlet hole pointed out with number 6. The inward channels will be etched free so they can bend easily. The window to release the channels is shown directly next to the sides of those channels in the light green.
A second design of the IP valve consist of giving each inward connection tube a separate inlet, shown in figure 6.3. The idea of this concept is that the inner cavity is also closing the individual tubes from each other by the silicon beams. The silicon beams are there to keep the plunger rigid when operated. So in theory different mediums could be used by mixing them in the valve itself.

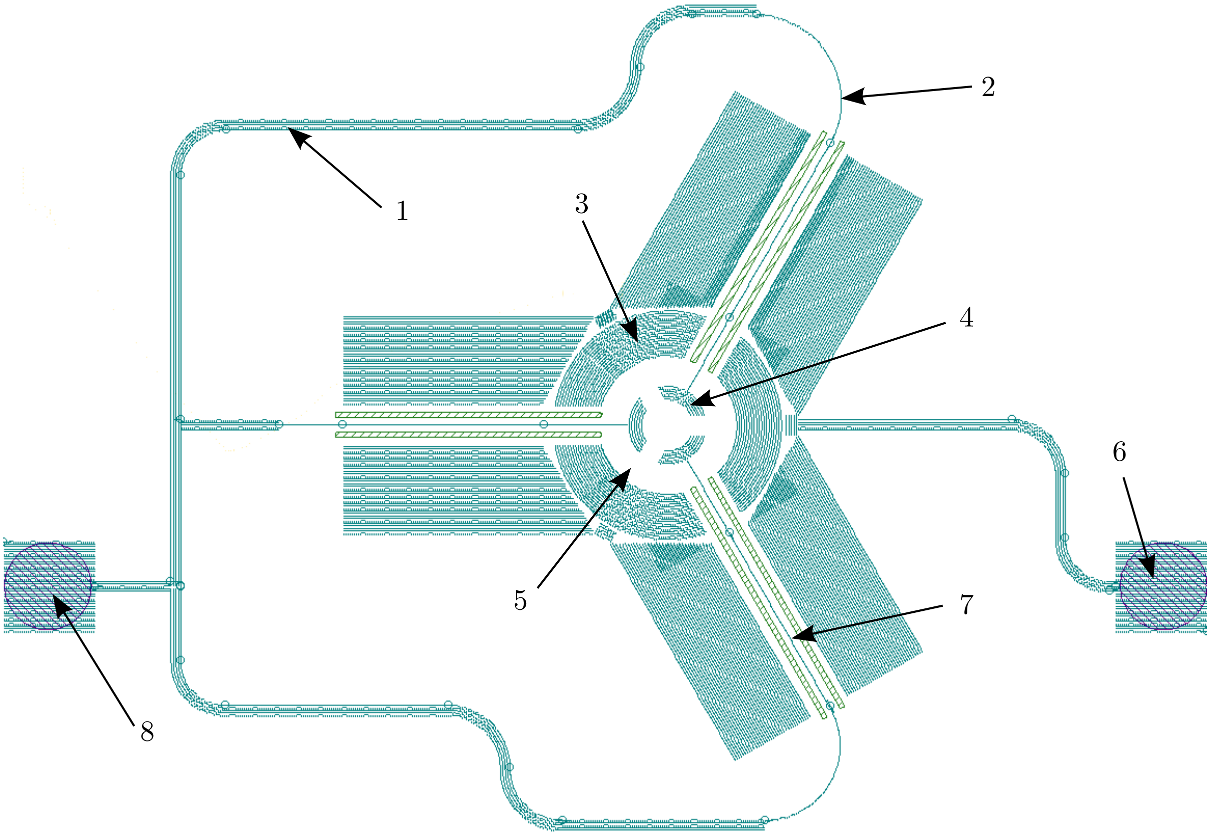

Figure 6.2: IP valve mask design, where the dark green is the slit mask, light green marks the release window mask and for the backetch the mask is shown in purple. 1) 5 slits wide channel 2) 1 slit wide channel 3) Slits for outer cavity 4) Slit pattern for inner cavity 5) Silicon plunger 6) Outlet hole 7) Free hanging inward tube in a tube 8) Inlet hole.

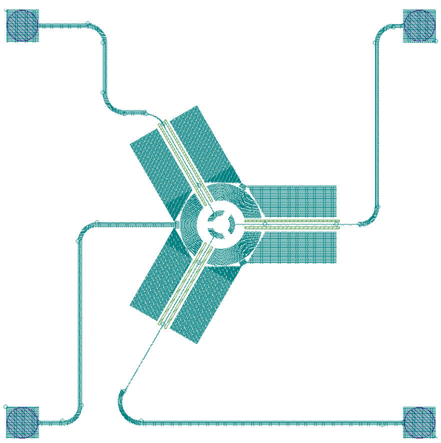

Figure 6.3: IP valve mask with separate connections to all tubes. The dark green represent the slit mask, light green marks the release window mask and for the backetch the mask is shown in purple.

7 Fabrication

During the fabrication of the valves some problems have occurred. These problems are analysed here to optimize the fabrication process to get a higher yield for next fabrication batches. First the exact process flow is discussed. Afterwards a look is taken at problems that occurred during the fabrication process.

7.1 Process flow

In figure 7.1 the important steps of the process flow are shown, the exact step at each number will be pointed out in the text below. In appendix A the complete process for the fabrication can be found. In step 1 the SOI wafer is shown, the SOI wafer is build up from a handle layer of 400 µm and a device layer of 50 µm with a 5 µm BOX layer in between. Step 2 is to grow a layer of 1 µm thick SiRN on top of the silicon wafer using Low Pressure Chemical Vapour Deposition (LPCVD). SiRN is used so that the stress caused by different expansion coefficients between silicon-nitride and silicon is reduced. By using SiRN the extra silicon atoms in the crystal lattice will behave more like silicon itself. Then we focus on the backside of the wafer to spincoat the resist on it. The resist is exposed with the mask for the backetched fluidic connection holes and developed. Then the holes can be etched by using three different etching processes. First the SiRN has to be etched using Deep Reactive Ion Etching (DRIE). During fabrication of the SOI wafers an oxide layer is left on the backside of the wafer of 4.5 µm, which is not polished away like the device layer. This oxide layer is kept on the backside to prevent that the stress of the BOX layer and the handle layer will bend the wafer. So this oxide layer also has to be removed using a different DRIE recipe before etching the silicon is possible. The silicon is etched away till the BOX layer using DRIE and the Bosch process of etching and depositing to create a straight channel. The backside resist is removed and the following process steps are preformed on the device layer.

A layer of chrome is sputtered to protect the SiRN from the following etching steps. Without the chrome mask the slits will become bigger, which is not desirable when they have to be closed again. Resist is spincoated on the chrome to pattern it with the slits to create the membrane and channels. Again using a DRIE recipe the thin layers of chrome and SiRN are removed. Using DRIE the silicon underneath the membrane is isotropic etched away, as is shown in step 3. With use of the spacing and several rows of slits parallel the depth of the channel can be tuned. So the depth of only one row of slits is not touching the BOX layer, whereas the parallel rows of slits can uncover the BOX layer completely.

Using Hydrogen Fluoride (HF) the BOX layer is etched away with an extra large underetch time at a rate of 1.4 µm min^{-1}. The added chrome layer protects the SiRN layer from the top side from the HF. The etchrate of SiRN with HF is 5 nm min^{-1}, so with an etchtime of 70 min this should mean 0.35 µm is etched away form the bottom of the SiRN layer. The underetch is needed to remove the BOX layer under the plunger for all designs and under the tube inside a tube concept for the IP valve. The BOX layer is etched in two steps to prevent sticking of the plunger to the seat, because of capillary forces occur when using a wet etchant. So when the left over BOX layer is around 5 µm to 10 µm the process is stopped. Now first the chrome is removed using a wet etchant and the wafer is cleaned, now the wafer looks like step 4. After cleaning the second step of etching the leftover oxide is done using vaporized HF. The valve will now not get sticked to the bottom, because there is no wet etchant which can cause a capillary force that results in sticking. Now in the remaining process no wet chemicals can be used inside the channels.

The second SiRN deposition step is used to cover the silicon wall in the channels and close the slits, which results in step 5. The deposited layer thickness is 1.5 µm. Because deposition occurs

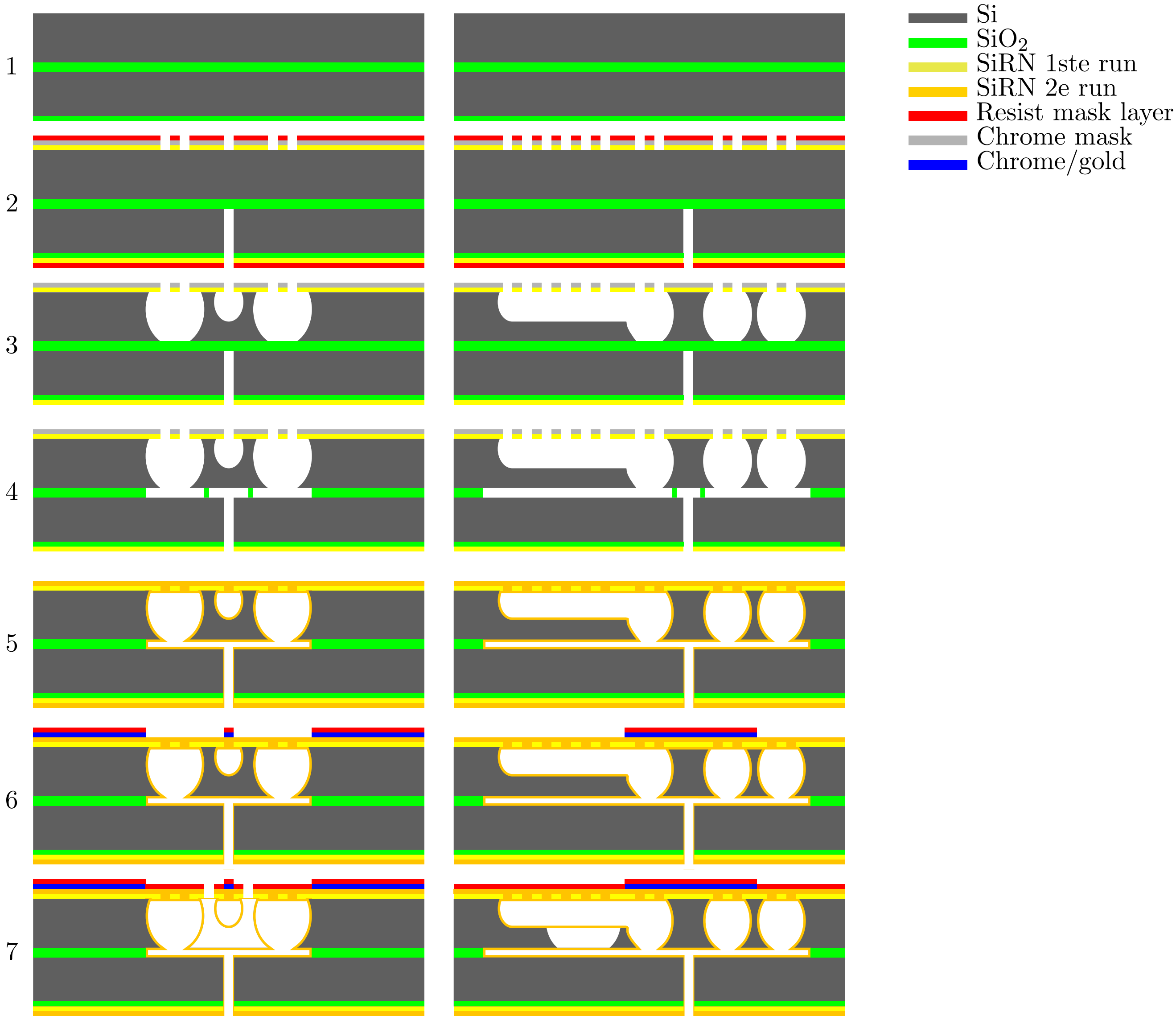

Figure 7.1: Process steps for the micro-Coriolis mass flow sensorand the BE and IP valves. On the left the crosssection of the tube in a tube concept is shown. On the right the plunger area can be seen with on the left a part of the inward channel. The scale doesn't match with the actual design.

on both sides the membrane will end up to be 3 µm thicker. The second SiRN layer prevents the plunger to make the maximum possible stroke of 5 µm. The deposition will be on both the plunger and seat, so twice the deposition thickness is lost leaving a stroke length of 2 µm.
For alignment markers for actuation and electrical connections for the micro-Coriolis mass flow sensor a metal layer is again deposited. First a layer of chrome is sputtered and afterwards a layer of gold. The chrome acts as adhesion between the SiRN and the gold. Resist is again spincoated and exposed. The resist has to be developed in a wet chemical. To prevent the wet chemical from entering the channels the backside is covered with dicing foil. The channels are closed accept for the backside, so by closing the inlets and outlets the channels stay dry. After spindrying the wafer the dicing foil is again removed. As is shown in step 6 the chrome and gold

layer are then etched away using Reactive Ion Beam Etching (RIBE). The resist is afterwards stripped using oxygen plasma, which is again a dry process step. In the final step of etching the release mask SU-8 is used as resist, because of the low temperature that prevents burning of the small tubes. Again dicing foil is used during development. Using several recipes for DRIE the release window for etching the silicon is made. The release in step 7 is only important for the IP valve and the micro-Coriolis mass flow sensor itself. The silicon is isotropic etched away to create free hanging channels. The free hanging channels are used to create a tube inside a tube to bridge the outer cavity. The SU-8 is stripped using O_2 plasma. With all these steps done the valve is ready to be broken into samples and measured.

7.2 Ruptured membrane at backetch hole

During the DRIE process for creating the channels the BOX layer between the backetch holes and the channel ruptures. Because the BOX layer is torn apart the shockwave also tears the SiRN membrane. At the backside of the wafer a helium pressure is present. The helium is used to cool the wafer during the etching process. Because of the back etched holes for the fluidic connection the helium can break through the thin oxide layer when the device layer is etched away. The tear might be closed again by the second SiRN grow step if it is small enough and aligned with the rest of the membrane.
A design on the same wafer with exactly the same connection holes but with a smaller cavity above the back etched hole didn't rupture. In figure 7.2 the large cavity is shown and in figure 7.3 the smaller cavity above the backetch hole is shown. The membranes are almost completely gone due to sawing the wafer into pieces for cross-section inspection. So to prevent tears in the SiRN membrane the cavity above the backetch hole has to be small. The cause of the rupture is the large surface area of the SiRN membrane. The large surface area causes a high force on it due to the shockwave pressure of the helium. But also the membrane is less stiff, because of the large area over which it can bend. So in future processing the area of the inlet cavity has to be small to prevent rupturing of the SiRN membrane.

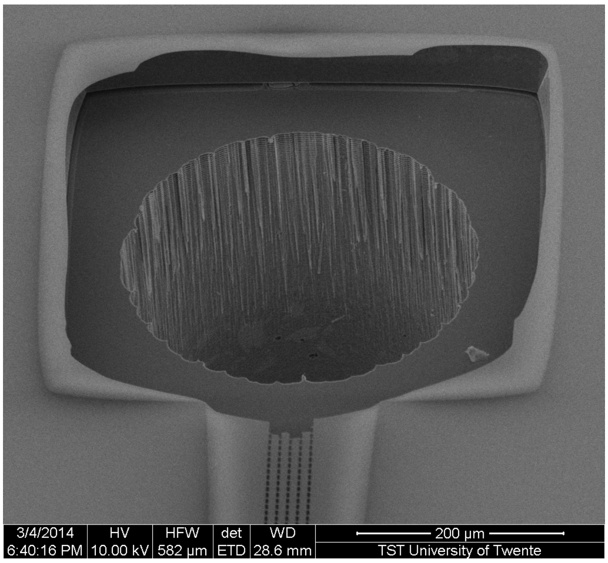

Figure 7.2: Inlet hole under large cavity

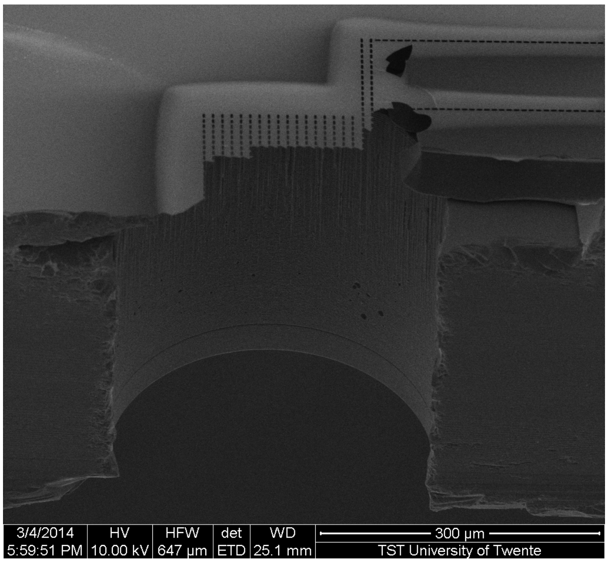

Figure 7.3: Inlet hole under small cavity

7.3 Torn membrane at sharp corners

In the IP valve design the membrane is torn at the point where the SiRN membranes from the tube in a tube membrane intersect. The sharp angle of the membrane at that point gives higher stress levels, which causes the membrane to tear at that point. Also this membrane crack might be closed in the second SiRN grow step. This means a weak point is created on the SiRN membrane, which could tear again by the induced force of the pressure underneath. To prevent the crack the sharp angle in the corners of the membrane have to be decreased, so less stress can build up.

7.4 Too large silicon etch time

For a better chance of a successful fabrication the wafer had two different designs to cope with imprecise etching time of DRIE of the silicon for the channels. The second designs was made with a failsafe, so that a longer etching time of the silicon would not destroy the valve. But during fabrication the etching time was even for the failsafe design too long, because the etching of the silicon in the inner cavity was less fast then was anticipated. So every silicon structure under the SiRN membrane apart from the inner cavity was too far overetched. In figure 7.4 the 5 slits wide channel is shown. The silicon etch time was so long that the silicon was etched away completely on top of the BOX layer. It was intended that the silicon etch should be stopped before it reaches the BOX layer. Because the BOX layer acts as an etching stop, the loading of the etchant inside of the channel is changed. So with the loading changed the etching of the side walls becomes faster and so its shape changes.
In figure 7.5 a close-up is shown from the tube that goes inwards to the inner cavity of the IP valve. Only the bottom curved part is seen of what should be a closed channel. Because of the large overetch time the silicon that should shape the channel is already etched away partly. The following step of the second layer of SiRN can't create a closed tube anymore, so the valve becomes useless. The inlet and outlet are now directly connected to each other without the valve in between.
A slower etching rate for the inner cavity then for the other patterns is a big problem. As stated

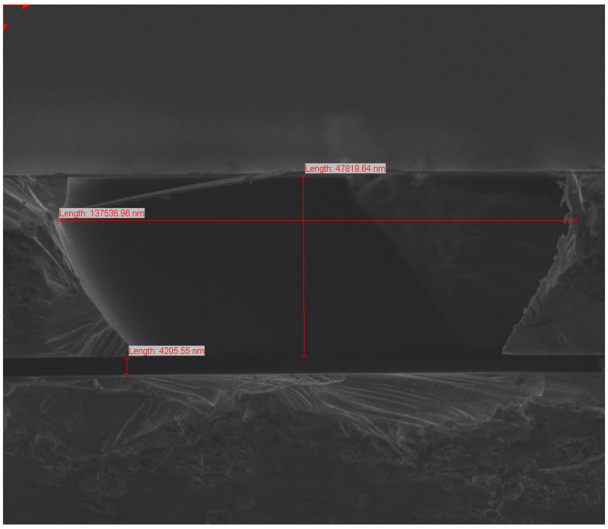

Figure 7.4: Overetched channel of 5 slits wide showing BOX layer was uncovered and removed during HF etch

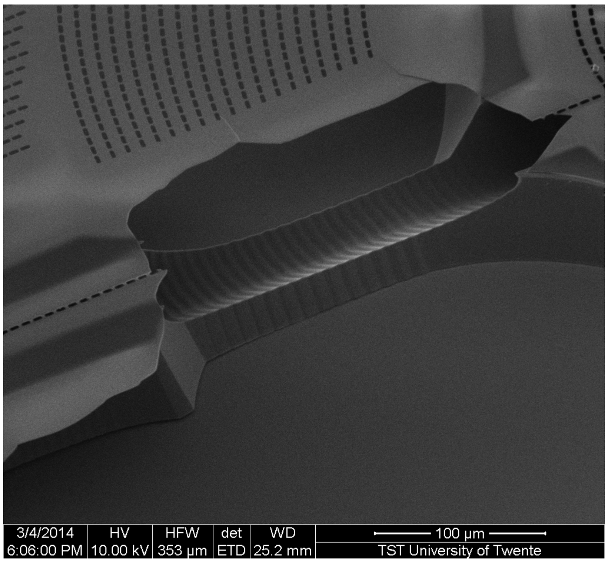

Figure 7.5: Close up of the inward tube for the in-plane fluidic channel showing only the bottom curve of the channel. All the other silicon is already etched away.

earlier the spacing between the rows of slits is a measure for the depth and also the speed of etching the silicon. Logically by making a more dense slit pattern the surface area for etching the inner cavity is increased. More etchant can penetrate later on through the slits and etch away the silicon much faster, so effectively decreasing the loading locally.

7.5 Haze on the wafer

After the channels are isotropic etched the BOX layer has to be removed. The mask consists of two layers on top of the SiRN, first a chrome layer to enhance the slit shape and second a resist layer. For etching of the oxide a solution of 50 % HF is used. After the HF etch the chrome mask is removed using chromium etchant. Afterwards the wafer should be clean, but that isn't the case. In the middle section the wafer looks clean, but further outwards a concentric haze is visible. The haze suggest there are still particles on the wafer or the SiRN surface is attacked and became rough. An Atomic Force Microscope (AFM) scan is done of the surface, which can be seen in figure 7.6. The surface is covered with pinholes of 150 nm deep, which is the cause of the haze. So the SiRN is indeed attacked through the chrome mask by the HF. In previous fabrication steps plasma is used for DRIE. The plasma inside the etching machine isn't uniform over the whole wafer. So probably the properties of chrome were changed, because in the middle of the wafer the plasma exposure was higher. This higher plasma exposure could cause that HF might penetrate the chrome in the middle less good then at the outside of the wafer.

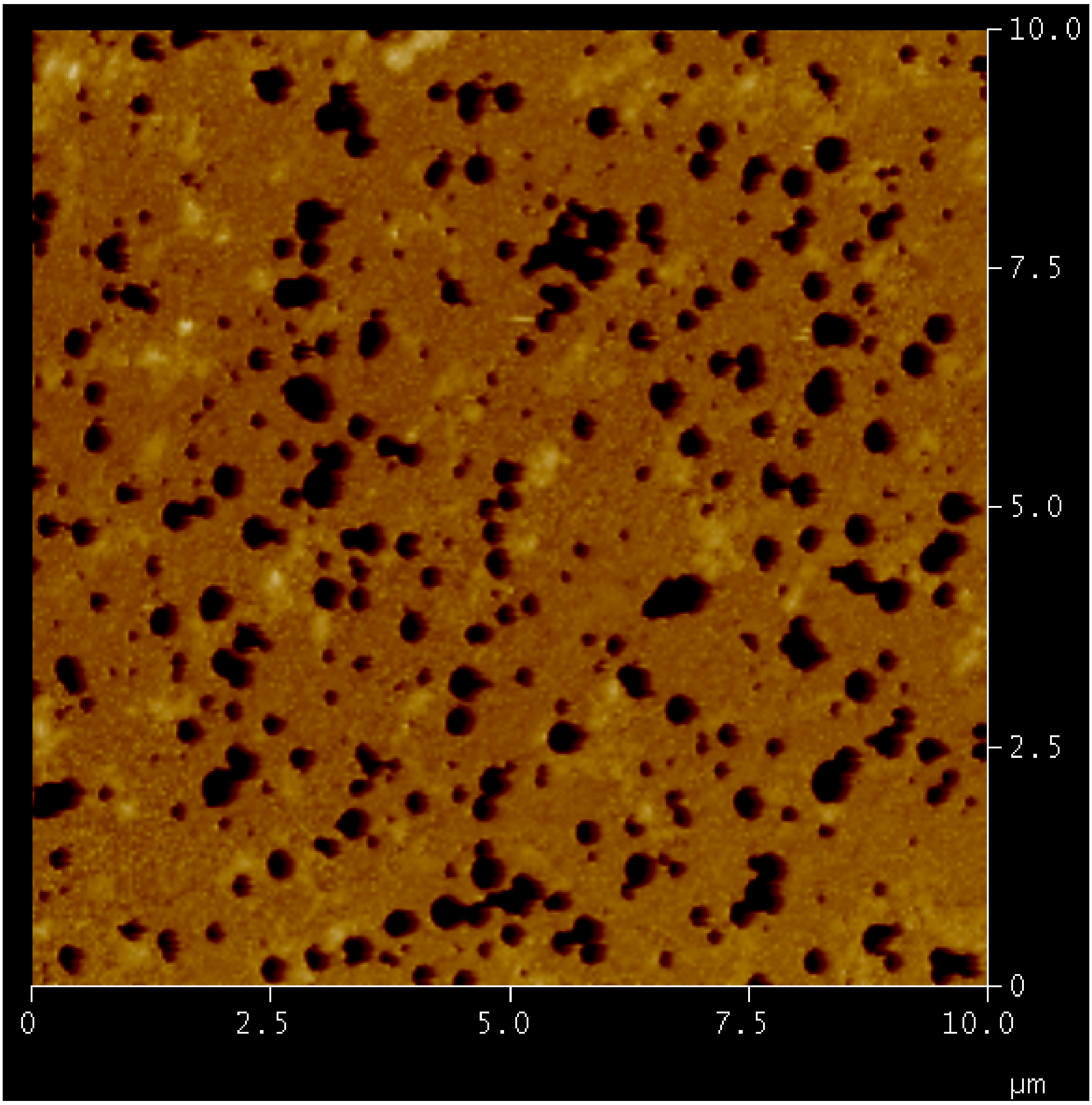

Figure 7.6: AFM scan of the wafer with a concentric haze showing the pinholes in the surface.

In the following process step of etching the last part of the BOX layer a vaporized HF is used. In this step also the wafer gets covered with a haze. After making an AFM scan and analysing the contents on the surface of the wafer it seems also that there are pinholes present in the

SiRN layer. So HF makes pinholes in the SiRN when this is used for etching.

7.6 Dirty wafer border

Another problem is a dirty border on the wafer. The border is an effect from the holder in which the wafer is clamped during the dry etching processes. Because the border is covered during mechanic clamping the wafer is not processed underneath at the same rate as the rest of the wafer. The chrome is not removed within the process steps following. With traces of chrome still on the wafer the processing can not be continued, because of possible contamination of the machine for growing the SiRN. To overcome this problem a different process has to be used, so electrostatic clamping can be used. With electrostatic clamping the border is not covered and is processed with the same rate as the inner section.

8 Measurements plan

To determine the characteristics of the valve a measurement setup is used. A piezo driver is used to actuate the valve using a thin rod. The driving structure is fitted with a loadcell to measure the force that acts on the rod. The measerument is done by using National Instruments LabVIEW. The total setup is shown in figure 8.1.

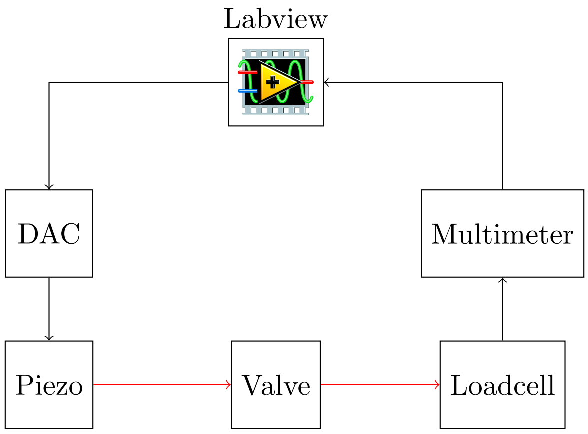

Figure 8.1: Block diagram of the measurement setup to determine the spring constant of the valve. Red arrows represent the mechanical domain and black arrows the electrical domain.

The springconstant of the valve can be determined by taking measurements of the displacement and the force that is used to actuate the valve. The displacement is calculated using the characteristics of the piezo. So the piezo is the driving element and the force is measured by the loadcell. Labview drives the piezo using a Digital Analog Converter (DAC). The loadcell outputs a voltage which is measured by a multimeter and read out by LabVIEW. Using the characteristics of the loadcell the exact force acting on the loadcell can be calculated. Knowing the force and the displacement the springconstant can be calculated.
The fluidic characteristics of the valve are also important. Because the membrane is rather thin the pressure of the medium can also push the valve more open. This could prove to be a good thing to overcome stiction problems when the valve is closed and won't open by itself. The rod that is attached to the piezo driver acts then also as the boundary, in such a way that the valve plunger is not exceeding its maximum stroke and the stress becomes so high that it breaks. For actively opening the plunger or for pulling it loose when it sticks the rod should be glued to the rod. This way the setup can be used to characterize the whole valve. To measure the flow through the valve it is connected to a fluidic network. The pressure controller is supplied with nitrogen gas from the lab facilities, which is at 10 bar. The pressure controller is given a setpoint using LabVIEW and then internally a valve and pressure sensor control the outlet pressure. The gas then passes a flow sensor before it runs through the valve, with its outflow to atmosphere. The setup is shown schematically in 8.2. With LabVIEW the data from the multimeter and the flow sensor are used to analyse the valve its characteristics.
Taking measurements of the flow at various plunger displacements should give a good overview of the fluidic characteristics. When the valve is closed completely the leakage between the seat and plunger has to be measured. SiRN is not a soft material that can close the channel completely, so there will always be a small leakage of the medium. Afterwards the stiction force can be measured by opening the valve by pulling with the piezo driver.

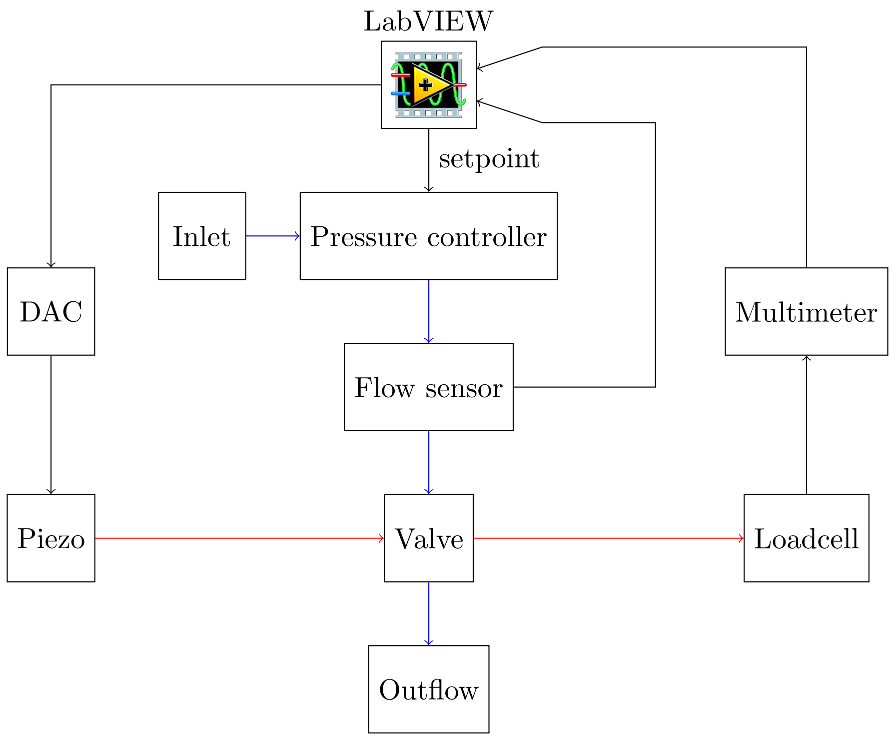

Figure 8.2: Block diagram of the measurement setup to determine fluidic characteristics. Red arrows represent the mechanical domain, black arrows the electrical domain and blue arrows the fluidic domain.

9 Discussion and Conclusion

Theoretical the designs of the backetched valve and the in-plane fluidic valve look promising. Where the backetched valve is a proof of concept for the functioning of the valve. The in-plane fluidic valve is the extended version of the backetched valve with the fluidic connections in-plane of the wafer. First the limits of the stress inside the membrane is determined. With the plunger having a maximum stroke of 2 µm due to the fact of the deposition of SiRN between the seat and plunger. The lowest possible stress is obtained for a membrane width of 200 µm. At this membrane width the stress inside the membrane stays under the 300 MPa, which is within a safe range for operating the valve. Also for the IP valve the tubes that go to the inner cavity acting as inlet have a stress lower as 300 MPa for bending till 4 µm, which is enough when the valve has to be closed or actively opened. The IP valve was simulated with the complete membrane including the mantle that is created by the tube in a tube concept. Also for this simulation the stress stays under the limit that was set. Another interesting fact is the force that is needed to actuate the valves. For the BE valve the force to close the valve is 24 mN. The IP valve needs less force to actuate, namely 7.5 mN. This is due the fact that the membrane is extended to suspend the outside of the tube in a tube concept.
Using COMSOL simulations the resistance reveals that the valve itself is dominant over the resistance of the inlet and outlet channels. So it is possible to use the valve to control the flow over the complete range of the mass flow the valves can pass. When the valves are actively pulled open with an opening of 4 µm the mass flow is $3\,\mathrm{g\,h^{-1}}$. With such a mass flow the valve satisfies the working range of the micro-Coriolis mass flow sensor, which is in the range of $1\,\mathrm{g\,h^{-1}}$.

9.1 Recommendations

Unfortunately due to several circumstances non of the wafers in process could be finished for measurements. So measurements of a functioning valve could not be made. But with observations during fabrication some improvements have to be made so a next fabrication run is successful. For a functioning in-plane fluidic valve the etching time for silicon during DRIE etching has to be tuned, so the inner and outer cavities are finished at the same time. For determining the etchrate of the BOX layer several structures at the outside of the wafer could be made to measure this, without destroying the wafer or several valves.
The process flow has to be slightly altered to ensure that the wafers stay clean. When the wafers are mechanically clamped for the dry etching processes the border is covered by the clamp itself. Because the border is covered it isn't processed as fast and on the same way as the rest of the wafer. After the etching is done and the wafer is cleaned a metallic ring on the outside border is left. With this metallic ring of chrome the wafer can't be used further for fabrication, because of contamination hazards in the fabrication machines. By using a different etching machine, which uses electrostatic clamping this problem can be solved. Another problem with the chrome mask is the SiRN layer which has a haze on it instead of the smooth finish after processing. The problem occurs during the etching step of dipping the wafer in 50 % HF with a chrome mask on top of it. The chrome mask should protect the SiRN, but instead the HF can penetrate the chrome mask and the same result is obtained after etching SiRN directly with vaporized HF.
During fabrication the membrane was torn at the backetch holes for the in and outlets. The problem was that the cavity above the backetch hole was to big. With a big cavity the membrane has a large surface area, which could not cope with the shockwave that occurred when the BOX layer broke because of the helium pressure underneath. By making the cavity smaller as was done on for other structures this problem doesn't occur anymore. In the design the membrane has a few sharp corners where the membrane is fixed. These sharp corners produce stress

concentrations at that point in the membrane, so tears appear in the membrane. To prevent these tears the corners have to be made less sharp in the mask design.
For the calculations of the fluidic part it is possible that the flow becomes turbulent in the first part of the radial channel. The turbulent part could be the explanation for the difference between the simulation and calculation. Also the artefact during simulation could therefore be a side effect of using the laminar flow module where the flow becomes turbulent. Because of time constraints this could not be researched further and has to be done in future work.
For future research in the working characteristics of the valves experiments have to be done to find out the possible stiction problems between the valve seat and plunger. Or by trying to search for a solution to reduce the stiction. The results can be used to improve the valve its performance and to up or downscale the design to alter its working area.
The actuation method has to be researched in more detail to produce a valve that can be used without an experimental setup. Therefore measurements between a coil and magnet have to be done to conclude if it is possible to use magnetic actuation. Or to come up with a design to use a bimorph material like a piezo to actuate the plunger.
To improve the position of the plunger a capacitive readout can be made by using the plunger or electrode on top of the plunger and the handle wafer as electrodes. This way a capacity is created, which can measure the position of the plunger.

A Fabrication process

Bibliography

[1] J. Haneveld, T. S. J. Lammerink, M. J. de Boer, R. G. P. Sanders, A. Mehendale, J. C. Ltters, M. Dijkstra, and R. J. Wiegerink, "Modeling, design, fabrication and characterization of a micro coriolis mass flow sensor," *Journal of Micromechanics and Microengineering*, vol. 20, no. 12, p. 125001, 2010.

[2] M. A. Dijkstra, M. J. de Boer, J. W. Berenschot, T. S. J. Lammerink, R. J. Wiegerink, and M. C. Elwenspoek, "A versatile surface channel concept for microfluidic applications," *Journal of micromechanics and microengineering*, vol. 17, pp. 1971–1977, September 2007.

[3] J. Groenesteijn, M. J. de Boer, T. S. J. Lammerink, J. C. Lötters, and R. J. Wiegerink, "Wafer-through access trenches for surface channel technology," in *1st International Conference on Microfluidic Handling Systems, Enschede, The Netherlands*, (Enschede), University of Twente, October 2012.

[4] G. Chung and K. Han, "Micromachined valves based on multilayer piezoelectric actuators," *Electronics Letters*, vol. 44, no. 18, pp. 1058–1060, 2008.

[5] T. Ohnstein, T. Fukiura, J. Ridley, and U. Bonne, "Micromachined silicon microvalve," in *Micro Electro Mechanical Systems, 1990. Proceedings, An Investigation of Micro Structures, Sensors, Actuators, Machines and Robots. IEEE*, pp. 95–98, 1990.

[6] COMSOL Multiphysics, Burlington, United States of America, *Finite element analysis, solver and simulation software package*, 2014. Available at http://www.comsol.com.

[7] E. I. Bromley, J. N. Randall, D. C. Flanders, and R. W. Mountain, "Technique for the determination of stress in thin films.," *Journal of Vacuum Science and Technology B: Microelectronics and Nanometer Structures*, vol. 1, no. 4, pp. 1364–1366, 1983. Cited By (since 1996):104.

[8] B. Kirby, *Micro- and Nanoscale Fluid Mechanics: Transport in Microfluidic Devices.* Cambridge University Press, 2010.

[9] The Engineering Toolbox, *Entrance Length and Developed Flow*, 2014. Available at http://www.engineeringtoolbox.com/entrance-length-flow-d_615.html.

[10] V. d. Browne and J. E. John, "Vacuum radial flow from the viscous through the free molecule regime," *Vacuum*, vol. 20, no. 12, pp. 525–533, 1970.

[11] D. Vokoun, M. Beleggia, L. Heller, and P. Šittner, "Magnetostatic interactions and forces between cylindrical permanent magnets," *Journal of magnetism and Magnetic Materials*, vol. 321, no. 22, pp. 3758–3763, 2009.

[12] PowerStream Technology, *Wire Gauge and Current Limits Including Skin Depth and Strength*, 2014. Available at http://www.powerstream.com/Wire_Size.htm.